Lawrence Berkeley National Laboratory
Recent Work

Title
ENHANCED INTERACTION IN THE POSITIVE COLUMN

Permalink
https://escholarship.org/uc/item/6pg1p47q

Author
Ecker, G.

Publication Date
1960-03-28

eScholarship.org Powered by the California Digital Library
University of California

UCRL 9144

UNIVERSITY OF
CALIFORNIA

Ernest O. Lawrence

Radiation Laboratory

ENHANCED INTERACTION IN THE POSITIVE COLUMN

TWO-WEEK LOAN COPY

This is a Library Circulating Copy which may be borrowed for two weeks. For a personal retention copy, call Tech. Info. Division, Ext. 5545

DISCLAIMER

This document was prepared as an account of work sponsored by the United States Government. While this document is believed to contain correct information, neither the United States Government nor any agency thereof, nor the Regents of the University of California, nor any of their employees, makes any warranty, express or implied, or assumes any legal responsibility for the accuracy, completeness, or usefulness of any information, apparatus, product, or process disclosed, or represents that its use would not infringe privately owned rights. Reference herein to any specific commercial product, process, or service by its trade name, trademark, manufacturer, or otherwise, does not necessarily constitute or imply its endorsement, recommendation, or favoring by the United States Government or any agency thereof, or the Regents of the University of California. The views and opinions of authors expressed herein do not necessarily state or reflect those of the United States Government or any agency thereof or the Regents of the University of California.

UCRL-9144

UC-20 Controlled Thermonuclear Processes
TID-4500 (15th Ed.)

UNIVERSITY OF CALIFORNIA

Lawrence Radiation Laboratory
Berkeley, California

Contract No. W-7405-eng-48

ENHANCED INTERACTION IN THE POSITIVE COLUMN

G. Ecker

March 28, 1960

Printed in USA. Price $1.25. Available from the
Office of Technical Services
U. S. Department of Commerce
Washington 25, D.C.

ENHANCED INTERACTION IN THE POSITIVE COLUMN

G. Ecker

Lawrence Radiation Laboratory
University of California
Berkeley, California

March 28, 1960

ABSTRACT

Recent theoretical work has shown that under certain conditions enhanced interaction may be present in a plasma. This paper investigates the influence of such enhanced interaction on the characteristics of the positive column in a longitudinal magnetic field. The calculations are based on the Boltzmann transport equations, using an effective interaction parameter. We find the following effects. From the law of momentum conservation we see that enhanced interaction causes enhanced diffusion by counteracting the influence of the magnetic field. Related to this is a pronounced influence on the radial potential distribution in the discharge. Both effects depend on the type of diffusion, showing characteristic differences between pure ambipolar diffusion, Simon diffusion, and intermediate types of diffusion. The law of particle conservation, which defines the electron temperature (T_-) in the discharge, is only indirectly - via the diffusion coefficient - influenced by enhanced interaction. This influence on the electron temperature is in general small. In particular it is shown that nonuniform enhancement may not affect T_- at all. Finally the law of energy conservation yields, for a given electron temperature, an increase in the ion (T_+) and gas (T_0) temperatures, and with that an increase in T_+/T_-. More important, it shows that the relation $X_z(T_-)$ between the electron temperature and the longitudinal electric field (X_z) is strongly affected by enhanced interaction. Utilization of these results suggests a new method to investigate experimentally the presence of enhanced interaction in the discharge. This method is based essentially on the measurement of the radial potential distribution.

ENHANCED INTERACTION IN THE POSITIVE COLUMN

G. Ecker*

Lawrence Radiation Laboratory
University of California
Berkeley, California

March 28, 1960

INTRODUCTION

The large interest that exists in the containment of charged particles by magnetic fields requires the understanding of the mobility and diffusion processes in the presence of magnetic fields. Certain experimental evidence[1, 2, 3] seemed to indicate diffusion losses across the magnetic field larger than could be expected according to simple collision theory.[4] An explanation of this phenomenon was first offered by Bohm with the concept of drain diffusion.[1] More recent theoretical investigations account for enhanced interaction and enhanced diffusion on the basis of microinstabilities.[5, 6, 7]

---

*Professor of Physics, Institute of Theoretical Physics, University of Bonn, Germany.

[1] D. Bohm, Characteristics of Electrical Discharge in Magnetic Fields, Edited by A. Guthrie and R. K. Wakerling, NNES.

[2] L. W. Davies, Proc. Phys. Soc. (London) 66, 33 (1953).

[3] W. H. Bostick and M. A. Levine, Phys. Rev. 97, 13 (1955).

[4] W. D. Allis, in Handbuch der Physik (Springer-Verlag, Berlin, 1956) 21, p. 383.

[5] L. Spitzer, Tech. Memo No. 50, NYO-7989, Princeton Univ., 1957.

[6] I. B. Bernstein, E. A. Frieman, R. M. Kulsrud, and M. N. Rosenbluth, Phys. Fluids, 3, 136 (1960).

[7] L. B. Bierman and D. Pfirsch, Cooperative Phenomena in Plasma Diffusion, Meeting of the Division of Plasma Physics, Monterey, 1959.

To furnish conclusive experimental evidence of enhanced diffusion, careful experiments on the positive column have been carried out by Bickerton and von Engel[8] and also by Lehnert.[9] These experiments are essentially based on the following idea:

If (X_z) is the axial electrical field component, n(r) the number density distribution, and μ_-, μ_+ respectively the mobilities of the electrons and ions, then the total discharge current (I) is given by

$$I = 2\pi (\mu_- + \mu_+) X_z \int_0^R n(r)\, r\, dr. \qquad (1)$$

On the other hand the law of particle conservation requires, in the absence of volume recombination,

$$L_w = 2\pi \cdot a \cdot T_-(X_z) \int_0^R \cdot n(r)\, r\, dr = -2\pi R \left(D_\perp \frac{dn}{dr}\right)_s, \qquad (2)$$

where L_w is the particle number wall loss per unit length of the column defined by the gradient dn/dr and the diffusion coefficient $D_\perp$ at the sheath edge near the wall (Index s), and $a(T_-)$ gives the number of ion pairs produced per electron and second as a function of T_-.

There follows from Eqs. (1) and (2) the relation

$$\frac{a[T_-(X_z)]}{(\mu_- + \mu_+)X_z} = \frac{L_w}{I}. \qquad (3)$$

As $a(T_-)$ increases rapidly with T_-, which in turn increases with X_z, it is obvious that an increase in the particle loss L_w must result in an increase of X_z. With the help of (2) and (3) the increase in X_z may be readily

---

[8] R. G. Bickerton and A. V. Engel, Proc. Phys. Soc (London) B, 69, 468 (1946).

[9] B. Lehnert, in Second International Conference on the Peaceful Uses of Atomic Energy, Geneva, 1958 (United Nations, New York, 1959) 32, p. 349.

related to the increase of $D_\perp$, if the following two assumptions are fulfilled: First, the enhancement of $D_\perp$ is uniform over the discharge cross section, then $(dn/dr)_s$ can be found from the Schottky theory. Second, the enhancement process does not influence the relation $T_-(X_z)$. Then only elastic and inelastic collisions with the neutral gas are important and $T_-(X_z)$ can be taken from experimental[8] or theoretical knowledge.[9]

In this way the experiments quoted above investigate the change of the diffusion coefficient $D_\perp$ by measuring the axial field X_z.

Bickerton and V. Engel[8] do not find indications of enhanced diffusion.

Lehnert,[9] however, reported an abnormal sudden increase of X_z for magnetic fields beyond a certain critical field value (B_c). This seemed to support the existence of enhanced diffusion due to "electromagnetic turbulence."[9]

New experiments by Allen, Paulikas, and Pyle[10] revealed that the column constricts at (B_c) and forms a helix spiraling in close contact with the walls of the tube. The phenomenon is similar to observations made by Elenbaas[11] for the high-pressure mercury vapor arc. This phenomenon provides an explanation for the voltage increase by the lengthening of the column and the influence of rotation, which causes a continuous transition into regions of low temperature.

---

[10] T. K. Allen, G. Paulikas, and R. V. Pyle, Instability of a Positive Column in a Magnetic Field, UCRL-9110 (in preparation).

[11] W. Elenbaas, High-Pressure Mercury Vapour Discharge, (North Holland Publishing Company, Amsterdam, 1951) p. 85.

OUTLINE OF THE PROBLEM

It is the aim of this investigation to study in detail the influence of enhanced interaction on the characteristics of the positive column for the following reasons:

Up to the present only the influence of a uniform increase of the diffusion coefficient $D_\perp$ on the longitudinal field X_z has been calculated under the assumption that $T_-(X_z)$ is unchanged.

As may be seen from the calculations,[5,6,7] the primary phenomenon in the discharge is "enhanced interaction." This produces as one of its results "enhanced diffusion," that is, an increase in $D_\perp$ --which, however, may be nonuniform over the discharge cross section, as the enhanced interaction depends on the density distribution. We wish to determine how such a nonuniform enhancement influences the particle conservation law, which defines the electron temperature in the discharge.

Moreover there are other pertinent consequences of enhanced interaction. In addition to the increase of the diffusion coefficient the enhancement process affects the energy exchange between electrons and ions and consequently the temperature conditions in the gas. We will show that the influence of enhanced interaction on the energy conservation law causes an increase in the ion and gas temperatures and deviations from the relation $T_-(X_z)$ as calculated without enhancement process.

The enhancement process influences the electric field X_z in a complicated way through the laws of momentum conservation ($D_\perp$), energy conservation $T_-(X_z)$, and particle conservation (T_-). One might raise the question whether there are other characteristics of the positive column that are influenced by enhanced interaction and might provide a suitable means for experimental study of this process. We will find, from the law of particle conservation, that the radial potential distribution is very strongly and characteristically dependent on the enhanced interaction, and might well provide an appropriate experimental tool to investigate this phenomenon.

The paper is divided into three parts, in which we calculate the influence of enhanced interaction on the law of conservation of particle numbers and momentum conservation and energy conservation, respectively. We base these calculations on the transport equations, which for an arbitrary quantity $V(\vec{v})$ read

$$\frac{\partial}{\partial t}(n\bar{V}) + \vec{\nabla}\cdot(n\overline{\vec{v}V}) - \frac{e}{m} n \overline{\vec{X}\cdot\vec{\nabla}_v V} + \frac{e}{m} n \overline{\vec{B}x\vec{v}\cdot\vec{\nabla}_v V} =$$

$$= \sum_i \int_{(8)} (V' - V)\, f_i(\vec{v}_i)\, f(\vec{v})\, c_i\, \rho_i\, d\Omega\, dv^3 dv_i^3, \qquad (4)$$

where f are the distribution functions, v the velocities, c the relative velocities, ρ_i the scattering functions. The quantities without indices refer to the particle under consideration, the index (i) to the other particle components with which the test particle collides. The prime (') characterizes quantities after collision. The bar indicates the v average.

PART I. THE LAW OF PARTICLE CONSERVATION

As is well known, the law of particle conservation follows from (4) by substituting V = 1, where ionization and recombination may be taken into account by using V' = 2 and V' = 0 respectively. The continuity equation

$$\frac{\partial n}{\partial t} + \vec{\nabla}\cdot(n\vec{v}_d) = n(a - a_r) \qquad (5)$$

simplifies for our application to a stationary state $(\partial n/\partial t = 0)$ without recombinations $(a_r = 0)$ to

$$\mathrm{div}\,(n\vec{v}_d) = an. \qquad (6)$$

Obviously enhanced interaction has an influence on this balance only over the drift velocity

$$v_d = \int_{(3)} \vec{v}\, f(\vec{v})\, d\vec{v}, \qquad (7)$$

which is studied in the next paragraph. There we show that $\vec{v}_d$ can be represented in the form

$$\vec{v}_d = - \frac{1}{n} \vec{\nabla} (D_\perp n) \qquad (8)$$

and that the enhanced interaction results in an increase of the diffusion coefficient D. Assuming enhancement uniform over the cross section one may consider $D_\perp$ constant, and Eq. (8) together with (6) yields by separation of the variables the Bessel-function solution of Schottky's theory, where the boundary conditions define

$$\alpha(T_-) = \left(\frac{2.4}{R}\right)^2 \cdot D_\perp \,, \qquad (9)$$

and with that T_-. The results of Part III on the energy conservation allows one then to determine the field X_z. The number of particles lost at the wall, L_w, may be taken from (3).

We notice that an increase in $D_\perp$ means only a moderate increase in T_- because T_- is logarithmically dependent on α, which again varies only porportionally to $D_\perp$. This makes the X_z measurements less sensitive.

However, even more restricting for the X_z measurements is the assumption of uniform enhancement. As enhanced interaction may depend on the particle density, it must be considered as a possibility that there is enhanced interaction in the center of the discharge, but less near the wall. Naturally this will cause deviations in the density distribution. However, unfortunately, this does not affect the electron temperature directly. Because T_- is defined only by $(dn/dr)_s$, and this quantity is little influenced by enhanced diffusion in the discharge center, the value of the electron temperature is virtually unaffected. To prove this we want to show in the following that L_w, T_-, and X_z change only very little, even if we assume an excessive increase of the diffusion coefficient over the major part of the discharge cross section.

It is difficult to solve the problem for an arbitrarily varying function $D_\perp(r)$. But to prove our assertion, we can easily evaluate the most unfavorable case, in which the diffusion coefficient ($D_\perp$) has been increased to $D_\perp \to \infty$ in the range $0 \leqslant r < r_0$ and is unchanged in the range $r_0 \leqslant r < R$ $(0 < r_0 < R)$. As is well known, the solutions in both regions

can be written in the form

$$n(r) = n_1' \cdot J_0(\gamma' r) + n_2' N_0(\gamma' r) \qquad \text{for } 0 \leqslant r < r_0, \tag{10a}$$

$$n(r) = n_1 \cdot J_0(\gamma r) + n_2 N_0(\gamma r) \qquad \text{for } r_0 \leqslant r < R, \tag{10b}$$

with

$$\gamma' = (a'/D_\perp')^{1/2}, \qquad \gamma = (a/D_\perp)^{1/2}, \tag{10c}$$

J_0 and N_0 respectively being the Bessel and Neumann functions of zero order.

The finite value of n at $r = 0$ requires $n_2' = 0$. For very large values of $D'_\perp$ ($D_\perp' \to \infty$) we have $\gamma' \to 0$, that means we find the solution

$$n(r) = n'_1 \qquad \text{for } 0 \leqslant r < r_0. \tag{11}$$

On the other hand we require, by the usual arguments (f. i.[12]) $n(R) \simeq 0$, and find

$$n_1 J_0(\gamma r) + n_2 N_0(\gamma r) = 0; \tag{12}$$

$n(r)$ must be continuous at r_0, and we have therefore

$$n_1 J_0(\gamma r_0) + n_2 N_0(\gamma r_0) = n'_1. \tag{13}$$

Also as $D_\perp\, dn/dr$ must be continuous at $r = r_0$, it follows

$$D_\perp'\ \gamma' n_1' J_1(\gamma' r_0) = D_\perp \gamma\ \{n_1 J_1(\gamma r_0) + n_2 N_1(\gamma r_0)\}, \tag{14}$$

which for $D_\perp' \to \infty$ yields

$$\frac{\gamma\rho}{2}\ n_1' = n_1 J_1(\gamma r_0) + n_2 N_1(\gamma r_0). \tag{14a}$$

---

[12] G. Ecker: Proc. Phys. Soc. (London) B 67, 485 (1954).

Eliminating n_1, n_2 and n'_1 from Eqs. (12), (13), and (14), we find the relation

$$\frac{J_0(x)}{N_0(x)} = \frac{J_1(\bar{x}) - \frac{\bar{x}}{2} J_0(\bar{x})}{N_1(\bar{x}) - \frac{\bar{x}}{2} N_0(\bar{x})} , \tag{15}$$

with

$$x = \gamma R \qquad \text{and} \qquad \bar{x} = x \cdot r_0/R. \tag{15a}$$

This Eq. (15) defines γ and with that T_- and X_z for given values of $D_\perp$, R and r_0. In the limit $r_0 = 0$ (15) simplifies to the usual condition (9).

For $r_0 \neq 0$ the solution of Eq. (15) can be obtained with sufficient accuracy by graphical methods. This problem is simplified by the fact that different parameter values r_0/R can be accounted for by a coordinate transformation. We have solved the equation for values $0 < r_0 < 0.85$ R.

The result is shown in Fig. 1, where we have plotted the value $x_r = x/x_0$ as a function of r_0/R. We note that the value of x_r does not depend on any special discharge data, such as ionization potential V_i, pressure p, excitation levels, etc. However, to find $T_{-r} = T_-/T_{-0}$ and $X_{zr} = X_z/X_0$ as a function of r_0/R, we have to know $a(T_-)$ and $T_-(X_z)$, which requires reference to definite discharge data. We have chosen as an example helium with $T_{-0} = 5 \times 10^4$ °K, and use $T_-(X_z)$ as calculated by Lehnert.[9] It should, however, be noted that according to our results in Part III a change of this relation in the presence of enhanced interaction must be expected.

Finally the relative number wall loss can be found, from Eqs. (3), (10c), and (15a), to be

$$L_{wr} = \frac{L_w}{L_{w0}} = \frac{x_r^2}{X_{zr}} . \tag{16}$$

All these quantities are plotted in Fig. 1 versus the parameter r_0/R limiting the region of enhanced diffusion. The results fully prove our assertion given above, since they show that even if we have an infinite diffusion coefficient ($D_\perp \to \infty$) for the main part of the discharge ($r_0 = 0.75$ R),

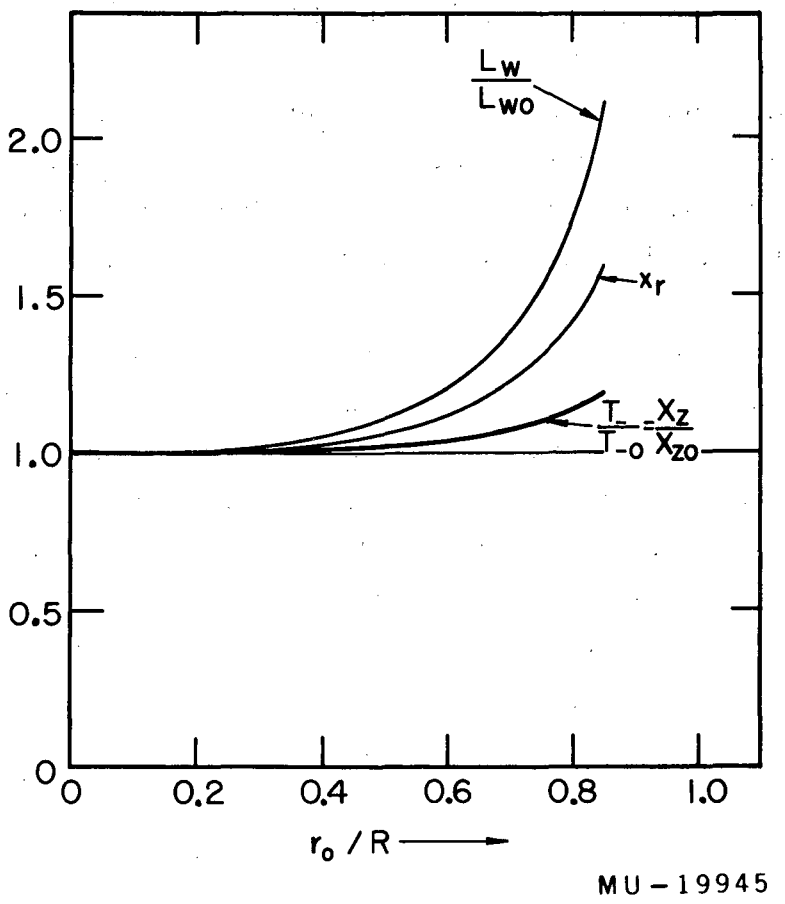

Fig. 1. This figure shows x_r, the solution of eq. (15) normalized to unity at $r_o = o$; L_w/L_{wo}, the relative wall loss; T_-/T_{-o}, the relative electron temperature; and X_z/X_{zo}, the relative longitudinal electric field as functions of r_o/r. Here r_o limits the region of enhanced diffusion ($D_\perp \to \infty$), R is the radius of the discharge tube.

the change in the longitudinal field strength (X_z) and the change in the electron temperature (T_-) amounts to only a few percent. An increase of $D_\perp \to \infty$ in the center part $r_0 = 0.4$ R would not be measurable, but fully overshadowed by the effect of the magnetic field on the diffusion coefficient $D_\perp$ in the range $r_0 < r < R$.

We conclude, therefore, that measurement of the electron temperature cannot conclusively eliminate the presence of enhanced diffusion in the discharge, because even under the extreme conditions discussed above (i. e., $D_\perp \to \infty$), enhanced diffusion over the major part of the discharge would hardly affect the T_- values. Whether X_z measurements may allow a conclusive check on the phenomenon depends on the influence of enhanced interaction on the relation $T_-(X_z)$, which will be studied in Part III.

One other point of interest may be noted in connection with the results of Fig. 1. That is that also the wall losses are only moderately influenced by enhanced diffusion as long as a small region near the walls is not affected. This feature--which, of course, is not limited to the special discharge under consideration--may be of interest for the problem of plasma confinement in a magnetic field.

PART II. THE LAW OF MOMENTUM CONSERVATION

The law of conservation of momentum follows from Eq. (4) if we identify V with mv. For the electron and ion component of our ensemble we obtain[13] the equations

$$\vec{B} \times \vec{\Gamma}_+ + \frac{\vec{\Gamma}_+}{\mu_+} + \eta e n (\vec{\Gamma}_+ - \vec{\Gamma}_-) = n \vec{X} - \vec{\nabla} \left(\frac{\overleftrightarrow{P}_+}{e} \right), \qquad (17a)$$

[13] W. P. Allis and S. J. Buchsbaum: Notes on Plasma Dynamics, Summer Program (1959) M. I. T.

$$-\vec{B} \times \vec{\Gamma}_- + \frac{\vec{\Gamma}_-}{\mu_-} + \eta e n \quad (\vec{\Gamma}_- - \vec{\Gamma}_+) = -n\vec{X} - \vec{\nabla}\left(\frac{\overleftrightarrow{P}_-}{e}\right), \qquad (17b)$$

where $\vec{\Gamma}_-$, $\vec{\Gamma}_+$ are the particle current densities and where we have

$$\overleftrightarrow{P}_\pm = \overleftrightarrow{p}_\pm + \vec{v}_{d\pm}\Big)\Big(\vec{v}_{d\pm} \quad m; \qquad (17c)$$

$\overleftrightarrow{p}$ is the normal pressure tensor, $\vec{v}_d$ the drift velocity; $\mu_\pm$ are the mobilities due to the interaction with the neutral gas only, η is the resistivity of a fully ionized gas.

These equations can be separated into components with respect to a cylindrical coordinate system. To find the radial distribution the z components are of no interest. The other equations read

$$\mu_+ B \Gamma_{\theta+} + \Gamma_{r+} + \sigma_+ (\Gamma_{r+} - \Gamma_{r-}) = n\mu_+ X_r - \frac{\partial}{\partial r}(nD_+), \qquad (18a)$$

$$-\mu_- B \Gamma_{\theta-} + \Gamma_{r-} + \sigma_- (\Gamma_{r-} - \Gamma_{r+}) = -n\mu_- X_r - \frac{\partial}{\partial r}(nD_-), \qquad (18b)$$

$$-\mu_+ B \Gamma_{r+} + \Gamma_{\theta+} + \sigma_+ (\Gamma_{\theta+} - \Gamma_{\theta-}) = n\mu_+ X_\theta - \frac{1}{r}\frac{\partial}{\partial \theta}(nD_+) \qquad (18c)$$

$$\mu_- B \Gamma_{r-} + \Gamma_{\theta-} + \sigma_- (\Gamma_{\theta-} - \Gamma_{\theta+}) = n\mu_- X_\theta - \frac{1}{r}\frac{\partial}{\partial \theta}(nD_-) \qquad (18d)$$

where we remember that $\mu_\pm$ is constant, and introduce the abbreviation

$$\sigma_\pm = e\eta\mu_\pm n \quad \text{and} \quad D_\pm = \mu_\pm \frac{P_\pm}{e} = \mu_\pm \frac{kT_\pm}{e} n, \qquad (19)$$

assuming that $P_\pm$ can be approximated reasonably by a diagonal tensor of constant scalar value $nkT_\pm$.

To Eqs. (18) we add the condition

$$\Gamma_{r-} = \epsilon \Gamma_{r+}. \qquad (20)$$

This condition covers at the same time the case of ambipolar diffusion ($\epsilon = 1$) and Simon diffusion ($\epsilon = 0$). For other values $0 < \epsilon < 1$ it is assumed that a fraction $(1 - \epsilon)\Gamma_{r+}$ leaves the discharge by Simon diffusion. Even the case in which the Simon contribution depends on the radial coordinate can be approximated within the range of Eq. (20) by a step solution.

Equations (18) and (20) are five expressions for the five variables X_r, Γ_{r+}, Γ_{r-}, $\Gamma_{\theta+}$ and $\Gamma_{\theta-}$.

If we add Eqs. (18a) and (18b) after multiplying by μ_- and μ_+ respectively, we eliminate X_r and obtain

$$\Gamma_{r+} = -\frac{\partial}{\partial r}\left[n\,\frac{\mu_- D_+ + D_- \mu_+}{\mu_- + \mu_+ \epsilon}\right] - \frac{\mu_+ \mu_- B}{\mu_- + \epsilon\,\mu_+}\,(\Gamma_{\theta+} - \Gamma_{\theta-}). \qquad (21)$$

Equations (18c) and (18d) allow us to express the azimuthal particle current densities $\Gamma_{\theta\pm}$ in terms of the radial particle current density Γ_{r+}. We have

$$\Gamma_{\theta+} = \frac{B\mu_+\,[1 + \sigma_+(1-\epsilon)]}{1 + \sigma_+ + \sigma_-}\,\Gamma_{r+}\,, \qquad (22a)$$

$$\Gamma_{\theta-} = \frac{B\mu_-\,[-\epsilon + \sigma_+(1-\epsilon)]}{1 + \sigma_+ + \sigma_-}\,\Gamma_{r+}\,, \qquad (22b)$$

or

$$\Gamma_{\theta+} - \Gamma_{\theta-} = \frac{B[\mu_+ + \epsilon\mu_-]}{1 + \sigma_+ + \sigma_-}\,\Gamma_{r+}\,. \qquad (23)$$

This last quantity is proportional to the azimuthal electrical current. Introducing Eq. (23) into (21) gives us the radial particle current density,

$$\Gamma_{r+} = -\frac{1}{1 + \dfrac{B^2\mu_+\mu_-}{1+\sigma_+ + \sigma_-}\cdot\dfrac{\mu_+ + \epsilon\,\mu_-}{\mu_- + \epsilon\,\mu_+}}\,\frac{\partial}{\partial r}\,n\left\{\frac{D_+\mu_- + D_-\mu_+}{\mu_- + \epsilon\,\mu_+}\right\}. \qquad (24)$$

The assumption is justified that the diffusion coefficients D_+, D_- as defined in (19), are constant or at most vary only slightly in comparison with the number density n(r) (Note μ_+, μ_- = const; also Part III). We may then write (24) in the form

$$\Gamma_{r+} = - D_0 \frac{\partial n}{\partial r} \quad . \tag{25}$$

Consequently the apparent diffusion coefficient for simultaneous ambipolar and Simon diffusion in the presence of magnetic fields, taking into account the electron-ion interaction, is given by

$$D_0 = \frac{\dfrac{D_+\mu_- + D_-\mu_+}{\mu_- + \epsilon\ \mu_+}}{1 + \dfrac{B^2\mu_+\mu_-}{1+\sigma_+ + \sigma_-} \cdot \dfrac{\mu_+ + \epsilon\ \mu_-}{\mu_- + \epsilon\ \mu_+}} \quad . \tag{26}$$

This formula shows that the diffusion coefficient always increases with increasing interaction (σ_-, σ_+). Enhanced interaction reduces the decrease of the diffusion coefficient caused by the magnetic field.

For the reasons set forth above we are also interested in the radial potential distribution. The radial field may be found by introducing Eqs. (25) and (22b) into (18b),

$$X_r = - \frac{\partial U}{\partial r} = - \frac{1}{\mu_-} \left[D_- + \right.$$

$$\left. \frac{\dfrac{D_+\mu_- + D_-\mu_+}{\mu_- + \epsilon\ \mu_+} \left[\dfrac{\mu_-^2 B^2 [\sigma_+(1-\epsilon) - \epsilon]}{1 + \sigma_+ + \sigma_-} - [\epsilon + \sigma_-(\epsilon - 1)] \right]}{1 + \dfrac{B^2\mu_+\mu_-}{1+\sigma_- + \sigma_-} \cdot \dfrac{\mu_+ + \epsilon\ \mu_-}{\mu_- + \epsilon\ \mu_+}} \right] \frac{\partial\ \ell n\, n}{\partial r} \cdot$$

(27)

The radial potential distribution calculated by integration of (28) and using (19) is

$$\frac{eU}{kT_-} = \frac{c_0 c_3}{c_5}\, n + \left(1 + \frac{c_0 c_1}{c_4}\right) \ell n\, n + c_0 \left(\frac{c_2}{c_5} - \frac{c_1}{c_4} - \frac{c_3 c_4}{c_5^2}\right) \ell n\, (c_4 + c_5 n) + C, \tag{28a}$$

where C is an arbitrary integration constant and $c_0, \cdots, c_5$ are defined as follows:

$$c_0 = \frac{D_{am}}{D_-} \quad \frac{\mu_- + \mu_+}{\mu_- + \epsilon \mu_+} \; ;$$

$$c_1 = -\epsilon(1 + \mu_-^2 B^2);$$

$$c_2 = e\eta\, \mu_- \left[1 - \left(2 + \frac{\mu_+}{\mu_-}\right)\epsilon + \mu_+ \mu_- B^2 (1-\epsilon)\right], \tag{28b}$$

$$c_3 = (1-\epsilon)\, e^2 \eta^2 \mu_- (\mu_- + \mu_+);$$

$$c_4 = 1 + \frac{\mu_+ \mu_- B^2 (\mu_+ + \epsilon \mu_-)}{\mu_- + \epsilon \mu_+} \; ;$$

$$c_5 = e\eta(\mu_+ + \mu_-);$$

and the abbreviations

$$D_{am} = \frac{\mu_+ D_- + \mu_- D_+}{\mu_+ + \mu_-} \; ; \quad \sigma_{0\pm} = e\eta\, \mu_\pm n(0); \quad u_\pm = \mu_\pm B \tag{28c}$$

are used. Introduction of (28b) in (28a) is not advisable, as it yields extremely messy expressions which cannot be simplified.

However, a more adequate general description can be achieved by remembering

$$\mu_- >> \mu_+, \tag{29}$$

and by disposing of the arbitrary constant C (by choosing U = 0 at r = 0). We then find, from (28),

$$\frac{eU}{kT_-} = a_1 \left(\frac{1}{x} - 1\right) - a_2 \ln x + a_3 \ln \frac{1 + \frac{a_4}{x}}{1 + a_4} \tag{30a}$$

with

$$x = n(0)/n ; \qquad a_1 = \left(1 + \frac{T_+}{T_-}\right)(1 - \epsilon)\,\sigma_{0+},$$

$$a_2 = \frac{1 + u_+u_-\left[\frac{\mu_+}{\mu_-} - \epsilon\,\frac{T_+}{T_-}\right]}{1 + u_+^2 + \epsilon\, u_+u_-} ;$$

$$a_3 = \left(1 + \frac{T_+}{T_-}\right) \frac{(1-2\epsilon)u_+^2 + \epsilon u_+u_- + u_+^4(1-2\epsilon+2\epsilon^2) + u_+^3u_-(\epsilon-1)^2\epsilon + u_+^5(\epsilon-1)/u_-}{1 + u_+^2 + u_+u_-\epsilon}$$

$$a_4 = \frac{\sigma_{0-} + \sigma_{0+}}{1 + u_+^2 + u_+u_-\epsilon} \tag{30b}$$

As may be seen from (30b), we do not neglect σ_{0+} in comparison to σ_{0-}, in spite of (28c) and (29). The reason is that in the presence of collective enhanced interaction $\sigma_{0+}/\sigma_{0-} = \mu_+/\mu_-$ may no longer be correct (see Part III).

We further note that the preceding integration also gives a good approximation in the case of varying $\eta(r)$, provided that the variation of η is appreciably smaller than that of $n(r)$. Rapid changes of η may be accounted for by step solutions similar to the procedure used in Part I.

Equation (30) is still too complicated to be discussed in general form. We consider therefore in the following the radial potential distribution for the two most important cases of pure ambipolar and pure Simon diffusion.

Results for any special combination may be readily taken from (30). We note, here, only that within certain limits the distributions for mixed diffusion (ϵ) at a magnetic field B are identical with those of ambipolar diffusion ($\epsilon = 1$) at a magnetic field $\bar{B}$, if $(B/\bar{B})^2 = \epsilon$ holds.

The Ambipolar Radial Potential Distribution

The ambipolar case is characterized by $\epsilon = 1$. Introducing this in (30) and observing (29), we find readily

$$\frac{eU}{kT_-} = -\frac{1 + u_+u_-\left(\frac{\mu_+}{\mu_-} - \frac{T_+}{T_-}\right)}{1 + u_+u_-} \ln x + \frac{u_+u_-\left(1 + \frac{T_+}{T_-}\right)}{1 + u_+u_-} \ln \frac{1 + \frac{\sigma_{0-} + \sigma_{0+}}{1 + u_+u_-}\frac{1}{x}}{1 + \frac{\sigma_{0-} + \sigma_{0+}}{1 + u_+u_-}} . \tag{31}$$

We demonstrate this dependence of U on $x = n_0/n$ in a semilogarithmic plot in Fig. 2.

According to Eq. (31) the potential distribution is essentially affected by the magnetic field (B), the electron-ion friction, η, and the ratio μ_+T_-/μ_-T_+.

Obviously U values can exist only in a certain area which is limited by two U curves, $U_0(x)$ and $U_\infty(x)$, corresponding respectively to magnetic field values $B = 0$ and $B \to \infty$. They are

$$\frac{eU_0(x)}{kT_-} = -\ln x, \tag{32}$$

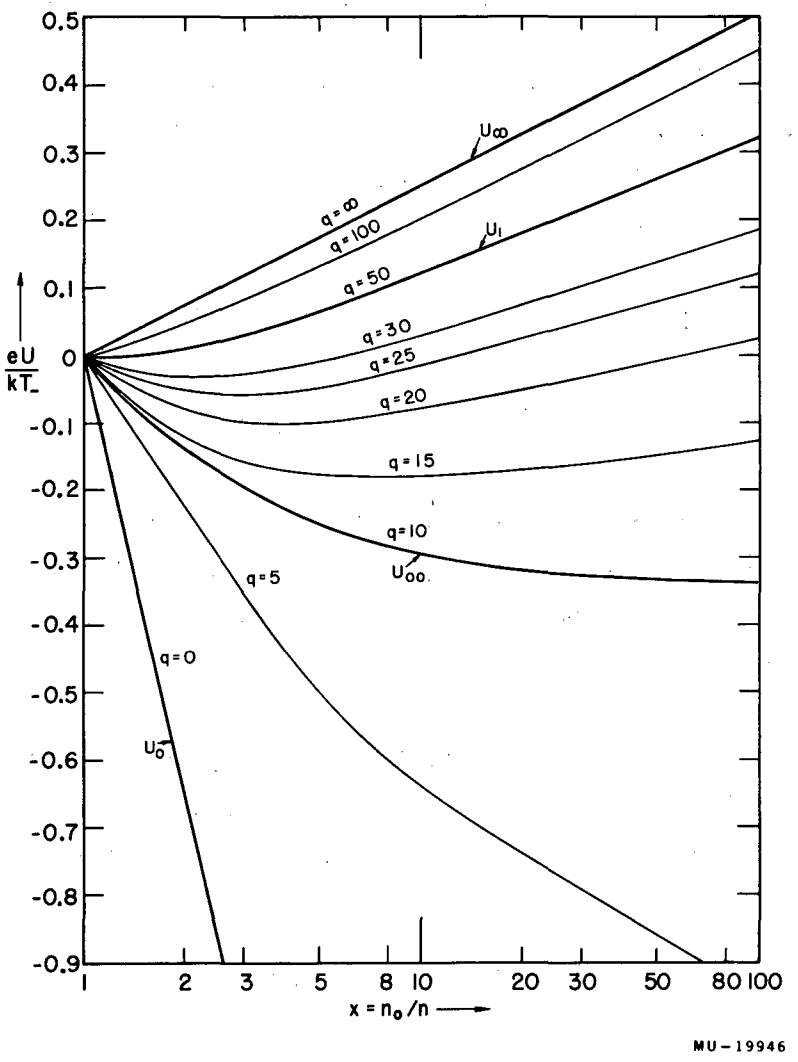

Fig. 2. This figure gives the ambipolar radial potential distribution (U) as a function of the density ratio $x = n_o/n(r)$ for parameter values of $q = u_+u_-B^2$ in the range $o \rightarrow \infty$.
$-\ \sigma_{o-} + \sigma_{o+} = 5 \cdot\ T_-/T_+ = 10.$

and

$$\frac{eU_\infty(x)}{kT_-} = \left(\frac{T_+}{T_-} - \frac{\mu_+}{\mu_-}\right) \ln x \quad . \tag{33}$$

In the semilogarithmic plot of Fig. 2 these relations are represented by straight lines, the lower limit U_0 being independent of the discharge conditions, the upper limit U_∞ being defined by $(T_+/T_- - \mu_+/\mu_-)$.

From Eq. (33) we see

$$U \lesseqgtr 0 \qquad \text{for } \mu_+ T_- \gtreqless \mu_- T_+, \tag{34a}$$

$$U \gtreqless 0 \qquad \text{for } T_+ \mu_- > T_- \mu_+. \tag{34b}$$

That means the ambipolar potential can never assume positive values--no matter how high we choose the magnetic field--if the relation (34a) holds. On the other hand, if equation (34b) is valid, then we can always arrive at positive potential values, if we choose the magnetic field B sufficiently strong.

This result is reasonable and can readily be understood from the diffusion coefficients of the electrons and the ions in the magnetic field. We would expect the sign of the ambipolar field to depend on the condition

$$D_{-B} = \frac{D_-}{1 + u_-^2} \gtreqless \frac{D_+}{1 + u_+^2} = D_{+B}, \tag{35}$$

which for large magnetic fields yields exactly the criterion

$$\frac{T_-}{\mu_-} \gtreqless \frac{T_+}{\mu_+} \quad , \tag{36}$$

as found from the general treatment above.

We understand further from Eq. (29) that the influence of the magnetic field becomes important as the value of the parameter $u_+ u_-$ approaches unity. For negligible electron-ion interaction, $\eta = 0$ the relation U(x) is simple because in the semilogarithmic plot all distributions are given by straight lines. The magnetic field affects only the slope of these lines.

The situation is more complicated when the influence of η is not negligible. Under all conditions the additional second term in Eq. (31) gives a negative contribution to U(x) and produces deviations from the straight lines. This effect is apparent in the curves of Fig. 2, which describe U as a function of the density $x = n_0/n$ for the case $T_+\mu_- > T_-\mu_+$. We have chosen this example because it applies to most of the experimental conditions encountered, and shows also the most conspicuous distributions. Of course, it is also desirable to know the potential distribution as a function of the radial distance from the discharge axis, U(r). This requires the knowledge of the density distribution n(r). Figure 3 shows U(r) as calculated from Fig. 2 by using $n(r) = n_0 \cdot J_0 \cdot (2.4\ r/R)$. Although this Bessel function might not describe the true density distribution in the discharge, this is unimportant. Figure 3 serves only as a means to demonstrate the principal features, and the conclusions we draw in the following hold for any density distribution n(r) that is monotonically decreasing towards the wall.

In Figs. 2, 3 we distinguish three different types of U curves. The first type occurs for small magnetic fields and is concave in the direction of the negative U axis. U values decrease steadily with increasing x or r. We encounter the second type of U curve when the magnetic field passes through the value B_0 given by

$$\frac{T_+}{T_-}\ \mu_+\mu_-\ B_0^2 = 1. \tag{38a}$$

Here the ambipolar potential first decreases, as for type 1, but at a certain $x_m(r_m)$ the potential passes through a minimum value and increases for $x > x_m(r > r_m)$. The position $x_m(r_m)$ is very large for magnetic fields close to B_0 and approaches the value $x_m = 1$ $(r = 0)$ for $B = B_1$, B_1 being defined by

$$\frac{T_+}{T_-}\ \mu_+\mu_-\ B_1^2 = 1+\sigma_{0-} + \sigma_{0+}. \tag{38b}$$

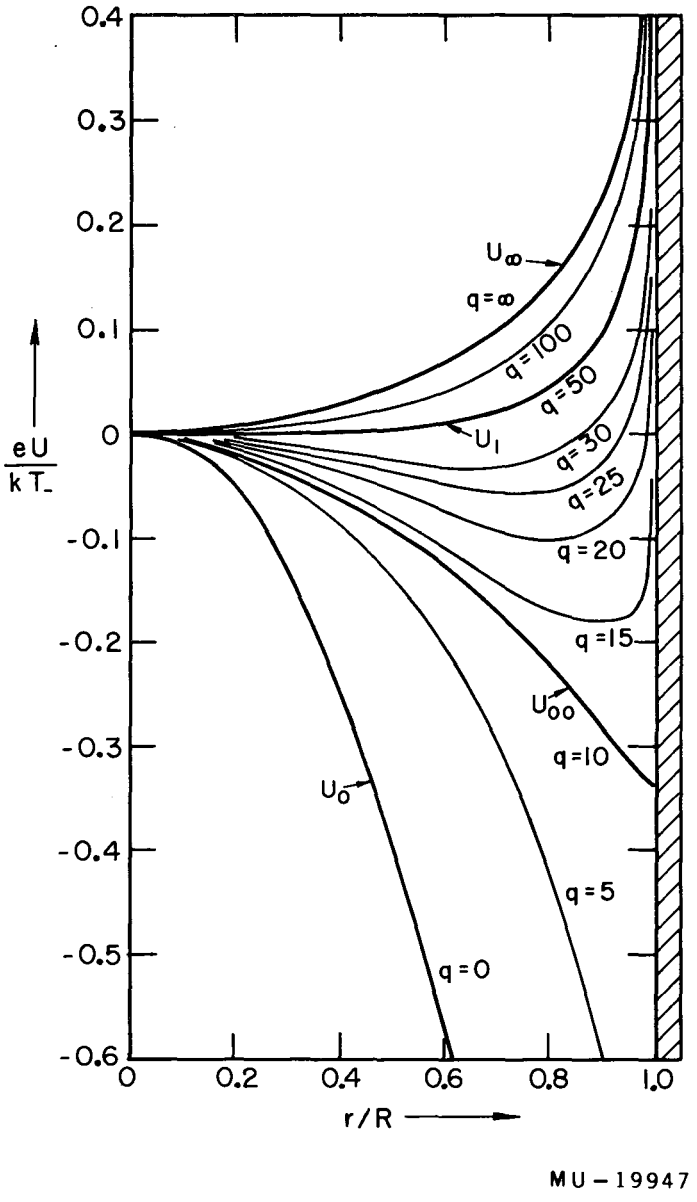

Fig. 3. The ambipolar radial potential distribution is plotted as a function of the relative radial distance r/R. The parameter values are identical with those in Fig. 2.

The point $x_m(r_m)$ of the potential minimum U_m may be called the "point of ambipolar field reversal". It is important to note that this phenomenon of field reversal is found only in a definite range of the magnetic field, limited by $B_0 < B < B_1$ defined in (38). The depth of the potential minimum decreases with increasing magnetic field. Finally, when B is greater than B_1 we have the third type of U curve, for which the U values increase steadily with x.

The preceding features may be readily understood by differentiating Eq. (31) and calculating the position x_m of the minimum, which yields

$$x_m = \frac{\sigma_{0-} + \sigma_{0+}}{\frac{T_+}{T_-} u_+ u_- - 1} \quad . \tag{39}$$

The Radial Potential Distribution for Simon Diffusion

Simon diffusion is characterized by $\epsilon = 0$. Introducing this into Eq. (31), we find the corresponding radial potential distribution,

$$\frac{eU}{kT_-} = -\ln x - \left(1 + \frac{T_+}{T_-}\right)\sigma_{0+}\left(1 - \frac{1}{x}\right) + \left(1 + \frac{T_+}{T_-}\right)u_+^2 \ln\left(\frac{1 + \frac{\sigma_{0-} + \sigma_{0+}}{1 + u_+^2} \frac{1}{x}}{1 + \frac{\sigma_{0-} + \sigma_{0+}}{1 + u_1^2}}\right). \tag{40}$$

Again we discuss separately the case without $(\eta = 0)$ and with $(\eta \neq 0)$ electron-ion-interaction.

If electron-ion friction is negligible the potential distribution assumes the extremely simple form

$$\frac{eU}{kT_-} = -\ln x. \tag{41}$$

The most striking feature of this case is that the distribution is independent of any discharge parameter--independent not only of the mobility and diffusion coefficient of the ions (μ_+, D_+), but also independent of the magnetic field. Moreover, comparison with (32) shows that the potential distribution for Simon diffusion with or without magnetic field is identical to the corresponding

ambipolar potential distribution without magnetic field, if we have $\mu_- >> \mu_+$ and $D_- >> D_+$.

These results can easily be made plausible. Without B, the ambipolar potential is given by

$$\frac{eU}{kT_-} = -\left(1 - \frac{D_{am}}{D_-}\right) \ln x = -\left(1 - \frac{D_+}{D_-} - \frac{\mu_+}{\mu_-}\right) \ln x, \qquad (42)$$

which approaches the discharge-independent distribution (41), as $D_+/D_- \to 0$. The reason for this is that for a small ratio of D_+/D_- the ambipolar field must almost completely compensate the electron diffusion to reduce Γ_{r-} to the small value of Γ_{r+}. The ambipolar field cannot therefore depend on D_+, as long as this is small in comparison with D_-. On the other hand, the ambipolar field does not depend on D_- either, because the mobility μ_- varies proportionally with the diffusion coefficient D_-. (The influence of T_- is shown in Eq. (42)).

As we require $\epsilon = 0$ for pure Simon diffusion, we have exactly the same conditions as in the ambipolar case $D_+/D_- \to 0$. Here too, the radial field must fully compensate the electron diffusion effect, and it is therefore not surprising that we find an identical distribution of U. The independence of the parameters D_+ and D_- follows in exactly the same manner as described in the preceding paragraph. And as D_+ and D_- do not influence the ambipolar field, the magnetic field B cannot have any influence on the distribution. One might think that the same argument would hold for the ambipolar case, requiring B independence for the ambipolar field too. This is not so, because with increasing B the condition $D_{0+}/D_{0-} << 1$ is violated. (See Eq. (26).)

The influence of friction contributes two terms, both always negative, one dependent on and the other independent of the magnetic field. In general the independent term

$$-\left(1 + \frac{T_+}{T_-}\right) \sigma_{0+} \left(1 - \frac{1}{x}\right) \qquad (40a)$$

is small in comparison with the main term (40) because $\sigma_0 << 1$. It is noteworthy that in the magnetic term,

$$-\left(1 + \frac{T_+}{T_-}\right) u_+^2 \ \ell n \ \frac{1 + \dfrac{\sigma_{0-} + \sigma_{0+}}{1 + u_+^2}}{1 + \dfrac{\sigma_{0-} + \sigma_{0+}}{1 + u_+^2} \ \dfrac{1}{x}}, \qquad (40b)$$

as should be expected, only u_+ but not u_- appears.

The radial potential distribution for pure Simon diffusion is shown in Fig. 4 as a function of $x = n_0/n$ and in Fig. 5 as a function of the radial distance r/R. Figure 5 was calculated on the same basis as described in connection with Fig. 3.

The Simon potential is always negative below the curve for Eq. (41) and concave towards the negative U axis. The limiting curves for B = 0 and B = ∞ are

$$\frac{eU_0}{kT_-} = -\ell n\, x - \left(1 + \frac{T_+}{T_-}\right) \sigma_{0+} \left(1 - \frac{1}{x}\right), \qquad (43a)$$

$$\frac{eU_\infty}{kT_-} = -\ell n\, x - \left(1 + \frac{T_+}{T_-}\right) (\sigma_{0+} + \sigma_{0-}) \left(1 - \frac{1}{x}\right). \qquad (43b)$$

Ambipolar Field Reversal as a Means of Detection of Enhanced Interaction

In the outline of this investigation we have raised the question whether there are other characteristics of the positive column that depend on the electron-ion interaction and may provide a suitable means for experimental detection of enhanced interaction. It appears that the results for the ambipolar potential distribution derived above can be used to obtain reliable information on η from measurements of the radial potential distribution. This may be seen as follows:

The equations (38a, b) yield immediately the relation

$$\sigma_{0-} + \sigma_{0+} = \frac{B_1^2 - B_0^2}{B_0^2}, \qquad (45)$$

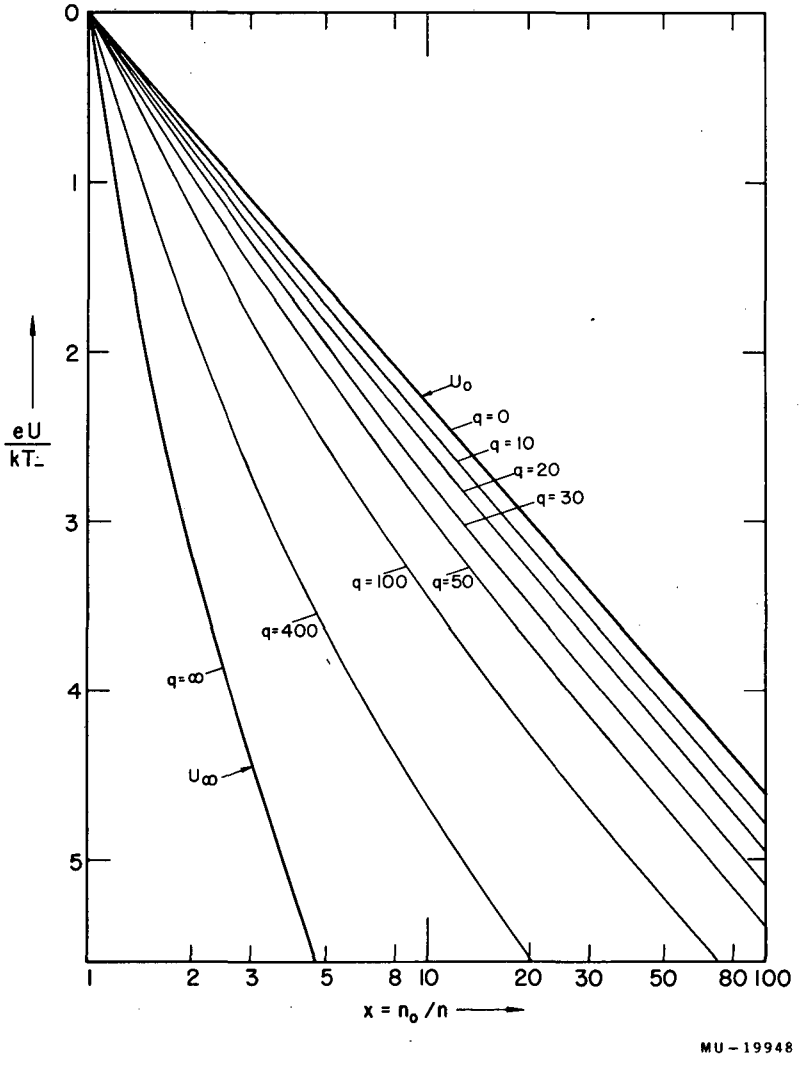

Fig. 4. The radial potential distribution for Simon diffusion (U) is given as a function of the relative density $x = n_o/n(r)$. The parameter values are identical with those stated in Fig. 2. In addition we have $\mu_-/\mu_+ = 10^2$.

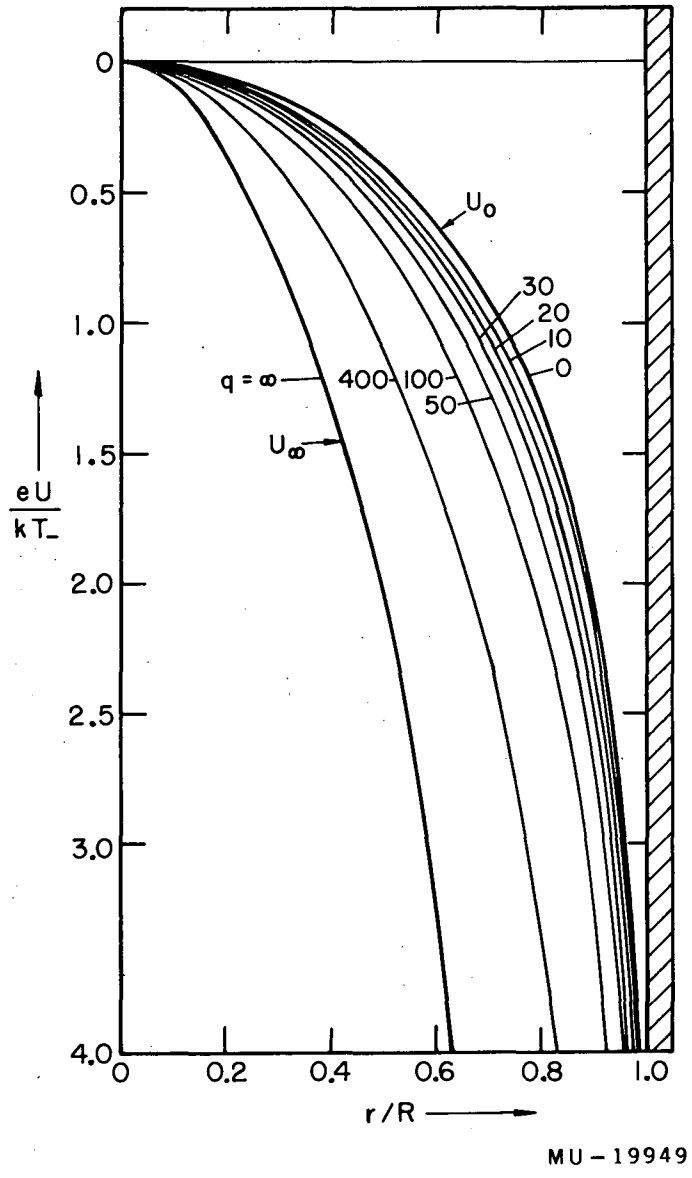

Fig. 5. The radial potential distribution (U) for Simon diffusion plotted versus the relative radial distance r/R. All conditions are identical with those of Fig. 3.

which offers a simple procedure to determine η_{exp}. We measure the lowest magnetic field B_0' for which we can reliably find field reversal, and we measure also the highest field B_1' for which we can still reliably see field reversal. Because of

$$B_0' > B_0, \qquad B_1' < B_1, \tag{46}$$

we then have

$$\sigma_{0-} + \sigma_{0+} \geq \frac{(B_1')^2 - (B_0')^2}{(B_0')^2}. \tag{47}$$

Accordingly, the presence or absence of enhanced interaction depends on whether in the following equation the (>) or the (=) sign holds:

$$\frac{(\sigma_{0-} + \sigma_{0+})_{exp}}{(\sigma_{0-} + \sigma_{0+})_{norm}} \geq \frac{(B_1')^2 - (B_0')^2}{(B_0')^2 e \cdot n_0 (\mu_- + \mu_+)\eta_{norm}}. \tag{48}$$

Here, η_{norm} designates the normal electron-ion interaction which, considering only individual Coulomb interactions, can be evaluated with the help of stochastic methods. The well-known result is[14]

$$\eta = 7.3 \cdot 10^{-9} \cdot \frac{\ell n \Lambda}{T^{312}}. \tag{49}$$

It may be mentioned that Eq. (48) includes relatively little uncertainty. The quantities e, $\mu_\pm$ are known with sufficient accuracy; η_{norm} is given by (49); B_0' and B_1' can be reliably measured because they refer to a rather conspicuous quality of the radial potential distribution, namely the point of field reversal. Knowledge of the density distribution n(r) is not required, as the distrubution U(r) must show field reversal for the same range of B values as U(x) because of the monotonic character of n(r). Only the maximum density n_0 in the center of the discharge enters the relation.

---

[14] L. Spitzer, Physics of Fully Ionized Gases (Interscience Publishers, New York, 1956), p. 84.

So far the argument is based on the assumption that T_-, T_+, and η are constant over the discharge cross section. This assumption may not hold because of a dependence of the enhancement process, that is of the "effective η," on the radial coordinate. We will show now that even in this case we may still use the procedure outlined above, provided that the variation of the effective η is small in comparison with the variation of n(r).

Again, let B_0'-B_1' be the range of magnetic fields for which the ambipolar potential goes to positive values near the walls and has a negative gradient $(dU/dx)_c$ at the center. From Eq. (31) it follows that positive potential values are possible only if we have

$$\left(\frac{T_+}{T_-}\ u_+u_-\right)_s > 1 \qquad (50)$$

near the wall. (Index s.)

On the other hand, differentiating Eq. (39) and requiring a negative gradient at the center ($(dU/dx)_s < 0$), we find

$$(\sigma_{0-} + \sigma_{0+})_c > \left(\frac{T_+}{T_-}\ u_+u_- - 1\right)_c . \qquad (51)$$

As may be seen from Part III, the ratio T_+/T_- increases with B and decreases with distance from the center towards the wall because $\sigma_{0-} + \sigma_{0+} = en\eta\,(\mu_+ + \mu_-)$ increases with B and decreases with increasing r under the assumptions stated above. Taking this into account and combining (50) at the field B_0', and (51) at B_1', we find again

$$(\sigma_{0-} + \sigma_{0+})_c > \frac{(B_1')^2 - (B_0')^2}{(B_0')^2} , \qquad (52)$$

which is identical with (47), only now restricted to the center (Index c).

Equation (52) is applicable, except when the variation of the enhancement parameter (effective η) with the radial coordinate is more pronounced than the density variation. However, it is still possible in this case to interpret the experimental results with the help of Figs. 2 through 5, using step solutions in suitable choosen intervals.

This last case demonstrates clearly that the procedure of measuring the radial potential distribution is appropriate for the study of enhanced interaction. Namely, if we consider the radial potential distribution for the experimental conditions underlying Fig. 1, Part I, we find that the enhancement ($D_\perp \to \infty$) in the range $0 < r < r_0$ has a very conspicuous effect on the potential distribution. As can be seen from (31), this distribution changes in the range $0 < r < r_0$ from

$$\frac{eU}{kT_-} = - \frac{1 + \left(\frac{\mu_+}{\mu_-} - \frac{T_+}{T_-} \right) u_+ u_-}{1 + u_+ u_-} \ln x \qquad (53a)$$

to

$$\frac{eU}{kT_-} = - \frac{1 + \left(\frac{\mu_+}{\mu_-} + 1 \right) u_+ u_-}{1 + u_+ u_-} \qquad \ln x \approx -\ln x. \qquad (53b)$$

Clearly this change will be detectable even if the range of enhancement limited by r_0 is so small that according to Fig. 1 there is practically no change in the longitudinal field gradient X_z.

Moreover, it should be noted that the procedure of measuring the radial potential distribution and the magnetic fields for ambipolar field reversal allows still another check on the presence of enhanced interaction. As was already mentioned, and is shown in Part III, the ratio T_+/T_- increases with increased electron-ion interaction. Now, using (50) at the magnetic field B_0', we have

$$\left(\frac{T_+}{T_-} \right)_{exp} > \frac{1}{(u_+ u_-)_0} \; ; \qquad (54)$$

If $(T_+/T_-)_{norm}$ defines the value of the temperature ratio expected for normal interaction conditions, then we have additional proof for enhanced interaction if we find

$$\left(\frac{T_-}{T_+}\right)_{norm} \cdot \frac{1}{(u_+ u_-)_0} > 1; \qquad (55)$$

$(T_+/T_-)_{norm}$ can be taken from the knowledge of pressure and electrical field (X_z).

PART III. THE LAW OF ENERGY CONSERVATION

As was indicated in the foregoing sections, we expect that enhanced interaction causes deviations of the temperatures (T_-, T_+, T_0) from those values which we would expect under normal conditions without enhancement process. In this section, therefore, we calculate the particle temperatures, taking into account electron-ion interaction.

To do so we start again from Eq. (4), substituting now $V = v^2$. This yields, for a stationary state, the relation

$$\vec{\nabla} \cdot \overline{n\vec{v}v^2} - \frac{2ne}{m} \vec{X} \cdot \vec{v}_d = \sum_i \int_{(8)} [(v')^2 - v^2] f_i(\vec{v}_i) f(v) \rho_i c_i \, d\Omega \, dv^3 dv_i^3, \tag{56}$$

where $\vec{v}_d$ is the drift velocity. In the most general case the scattering function ρ_i must be considered as a sum,

$$\rho_i = \rho_{0i} + \sum_x \rho_{xi}, \tag{56a}$$

where ρ_{0i} accounts for the elastic and ρ_{xi} for the inelastic collisions. For the elastic collisions we express the integrand as usual with the help of the relative velocities and the velocity v_g of the center of gravity,*

$$(v')^2 - v^2 = \frac{2m_i}{m+m_i} \vec{v}_g \cdot (\vec{c}_i' - \vec{c}_i) \tag{57}$$

and using the collision frequency in the center-of-gravity system, defined as

$$\nu_{gi} = n_i \int c_i \rho_{i0} (1 - \cos \chi_g) \, d\chi_g, \tag{58}$$

we have

---

*see, for instance, Ref. 4

$$\int_{(2)} [(v')^2 - v^2]\, d\Omega = -\frac{2m_i}{m+m_i}\ \frac{\nu_{gi}\ \vec{v}_g \cdot \vec{c}_i}{n_i}\ , \tag{59}$$

and, with that,

$$\int_{(8)} [(v')^2 - v^2]\ f(\vec{v}_i)\ f(\vec{v})\ c_i\ \rho_{i0}\ d\Omega\, dv^3 dv_i^3 =$$

$$= \frac{2m_i n}{(m_i+m)^2} \left\{ m_i \overline{v_i^2} - m\overline{v^2} \right\} \nu_{gi} \quad . \tag{60}$$

With respect to this last integration it should be mentioned that in general the collision frequency ν_{gi} depends on the velocities. However, in Eq. (60) ν_{gi} has been replaced by a constant average value, similar to the procedure and justification given by Allis and Buchsbaum[13] for the case of the momentum balance.

Introducing the collision frequency for momentum transfer in the laboratory system by

$$\nu_i = \nu_{gi}\ \frac{m_i}{m+m_i}\ , \tag{61}$$

we find

$$\int_{(8)} [(v')^2 - v^2]\ f_i(\vec{v}_i)\ f(\vec{v})\ c_i\ \rho_{i0}\ d\Omega\, dv^3 dv_i^3 = \frac{2\nu_i}{m_i+m}\ n \left\{ m_i \overline{v_i^2} - m\overline{v^2} \right\} . \tag{62}$$

For inelastic collisions we use

$$(v')^2 - v^2 = -\frac{2e}{m}\ V_{xi}\ , \tag{63}$$

and with the inelastic collision frequency

$$\nu_{ix} = n_i \int \rho_{ix}\ c_i\ d\Omega, \tag{64}$$

it is

$$\int_{(8)} [(v')^2 - v^2]\, f_i(\vec{v}_i)\, f(\vec{v})\, c_i \sum_x \rho_{ix}\, d\Omega\, dv_i^3\, dv^3 = -n \sum_x \nu_{ix} V_{ix} \frac{2e}{m} . \tag{65}$$

Introducing Eqs. (65) and (62) into (56) results in

$$\vec{\nabla} \cdot \overline{n\vec{v}v^2} - \frac{2ne}{m} \vec{X} \cdot \vec{v}_d = \sum_i \frac{2\nu_i n}{m_i + m} (m_i \overline{v_i^2} - \overline{mv^2}) - \sum_{i,x} \frac{n\nu_{ix} V_{ix} 2e}{m} . \tag{66}$$

Now, to eliminate $\vec{X}$, we again use Eq. (4), choosing $V = v$. We find

$$-\frac{ne}{m} (\vec{X} - \vec{B} \times \vec{v}_d) + \vec{\nabla} \overleftrightarrow{\overline{vv}}\, n = \sum_i \nu_i (\vec{v}_{id} - \vec{v}_d) n - \sum_{i,x} \nu_{ix} \vec{v}_d , \tag{67}$$

remembering

$$\int_{(2)} (\vec{v}' - \vec{v}) c_i \rho_{i0}\, d\Omega = \frac{m_i}{m + m_i} \int (\vec{v}_i - \vec{v})(1 - \cos\chi_g) c_i \rho_{i0} d\chi_g = \frac{\nu_{gi} \cdot m_i}{m + m_i} (\vec{v}_{di} - \vec{v}_d),$$

(68)

and using (56a) and (61). Again a constant average value for the collision frequency is used.

Substituting X from (67) into (66), we find

$$\sum_i \frac{2\nu_i nm}{m_i + m} \overline{(v^2 - v_d^2)} = \sum_i \left[\frac{2\nu_i n m_i}{m_i + m} \overline{(v_i^2 + v_d^2)} - 2n\nu_i \vec{v}_{id} \cdot \vec{v}_d \right] +$$

$$+ \sum_{ix} (2n\nu_{ix} v_d^2 - 2n\nu_{ix} \frac{e}{m} V_{ix}) - \vec{\nabla} \cdot \overline{n\vec{v}v^2} + 2\vec{v}_d \cdot \vec{\nabla} \cdot \overleftrightarrow{\overline{(vv)n}}.$$

(69)

Here the last term is negligible in comparison with the second-to-last term, because the drift velocity is practically perpendicular to the divergence of the pressure tensor. The random energy of the particles under consideration is

$$T_k = \frac{m_k}{2} \left(\overline{v_k^2} - v_{dk}^2\right). \tag{70}$$

Introducing this into (69) yields

$$T \cdot \sum_i \frac{\nu_i m}{m+m_i} = \sum_i \nu_i \left[\frac{m}{m+m_i} \frac{mv_d^2}{2} + \frac{m}{m+m_i} \frac{m\overline{v_i^2}}{2} - \frac{m}{2} \vec{v}_{id} \cdot \vec{v}_d\right] +$$

$$+ \sum_{ix} \nu_{ix} \left(\frac{v_d^2 m}{2} - \frac{eV_{ix}}{2}\right) - \frac{1}{4} \frac{\vec{\nabla} \cdot m n \overline{\vec{v} v^2}}{n}. \tag{71}$$

We may now use this general formulation to get information about the temperature of the ions (T_+), electrons (T_-), and neutral particles (T_0) in our discharge. In each case simplifications of Eq. (69) are possible.

First of all it seems sufficient to calculate for all particles only the temperature T averaged over the discharge cross section. This is true because we expect the quantities T_-, T_+, and T_0 to be nearly constant over the discharge diameter, which may be seen as follows.

For low values of σ_-, σ_+ the value of T_- is governed by the field X_z and the collision frequency with the neutral gas atoms (ν_{-0}). X_z must be independent of r because of $\vec{\nabla} \times \vec{X} = 0$ and the cylinder symmetry of the problem. ν_{-0} is constant because of the uniform neutral gas density. Consequently T_- should be independent of the radial coordinate. Again for small $\sigma_{-,+}$ the ion temperature must be constant, as it is defined only by the field X_z, the electron temperature T_-, and the collision rate with the neutral gas, all independent of r. Finally the neutral gas temperature T_0 must be practically constant, as the time rate of energy loss per unit area of the wall is small in comparison with the energy flux represented by the divergence term in Eq. (71).

The situation changes, however, with increasing σ_-, σ_+. Judging from (71) one might assume that T_- and T_+ show now a radial dependence because of the radial dependence of σ_-, σ_+. However, this conclusion would be incorrect, because values of σ_-, σ_+ necessary to produce a temperature effect ($\sigma_-, \sigma_+ \gtrsim 1$) occur only in the range of enhanced collective interaction. But under these conditions Eq. (71) should actually include an additional term of energy exchange between like particles, which tends to establish a temperature distribution uniform over the discharge cross section. The cause for this additional term can be readily understood. Going back to the Boltzmann equation, one sees that the relation (4) should in principle include in the summation of the right-hand side also a term accounting for the collisions of like particles. However, as is well known, this term cancels out in consequence of the conservation of momentum and energy in an individual collision. But as soon as collective phenomena come into play in the presence of enhanced interaction, this term is no longer zero and must be added to (71). The same mechanism that enhances the electron-ion interaction, $\sigma_{-,+}$, also increases the ion-ion and electron-electron interactions, therefore counteracting any appreciable temperature gradient of T_+, T_-.

Let us then average (71) over the cross section by multiplying with $2\pi r dr$, integrating from $0 \rightarrow R$, and dividing by the total particle number, $\pi R^2 \langle n \rangle$. Using Gauss's theorem for the divergence term, we arrive at

$$\langle T \rangle \sum_i \frac{\langle \nu_i \rangle m}{m_i + m} = \sum_i \langle \nu_i \rangle \left[\frac{m_i}{m + m_i} \left\langle \frac{m v_d^2}{2} \right\rangle + \frac{m}{m + m_i} \left\langle \frac{m \overline{v_i^2}}{2} \right\rangle - \frac{m}{2} \left\langle \vec{v}_{id} \cdot \vec{v}_d \right\rangle \right]$$

$$+ \sum_{i,x} \langle \nu_{ix} \rangle \left\{ \left\langle \frac{m v_d^2}{2} \right\rangle - \frac{e V_{ix}}{2} \right\} - \frac{m}{2R \langle n \rangle} (n \overline{\vec{v} v^2})_w \quad . \qquad (71a)$$

Here we have applied

$$\langle T\nu \rangle \simeq \langle T \rangle \langle \nu \rangle \; ; \; \langle \nu \rangle \left\langle \frac{m v_k^2}{2} \right\rangle \simeq \left\langle \nu \; \frac{m \overline{v_k^2}}{2} \right\rangle \; ,$$

making use of the fact that the temperatures are, in comparison with n(r), only moderately varying with radial distance. The index $(\ )_w$ designates values at the discharge wall.

Although in all future formulas we shall be using average values, for convenience we shall omit the symbol $\langle\ \rangle$.

We first discuss the ions ($m = m_+$). As was already stated, the main energy loss of the ions is due to the interaction with the neutral gas. In comparison with this the wall loss, represented by the last term in (71a), may be safely neglected. The electron mass is negligible compared with the ion mass ($m_- \ll m_+$), and for the same reason we have $m_0 \approx m_+$. Ions perform practically no inelastic collisions ($\nu_{+x} = 0$). The drift velocity of the neutral gas is zero ($v_{d0} = 0$). With this we deduct from (71) for the ions the relation

$$T_+ = \frac{m_+ v_{d+}^2}{2} \frac{1 + \frac{2\nu_{+-}}{\nu_{+0}} \left\{ \frac{m_-}{m_0} + \frac{v_{d-}}{v_{d+}} \right\}}{1 + \frac{2\nu_{+-}}{\nu_{+0}}} + \frac{m_0 \overline{v_0^2}}{2} \frac{1 + \frac{2\nu_{+-}}{\nu_{+0}} \frac{m_- \overline{v^2}}{m_0 \overline{v_0^2}}}{1 + \frac{2\nu_{+-}}{\nu_{+0}}} . \tag{72}$$

As can be readily verified from the foregoing, the quantities ν_{+-}, ν_{+0} are related to η, μ_+, μ_- by

$$\eta = \frac{m_+ \nu_{+-}}{e^2 n} = \frac{m_- \nu_{-+}}{e^2 n} \quad ; \quad \mu_+ = \frac{e}{m_+} \frac{1}{\nu_{+0}} \quad ; \quad \mu_- = \frac{e}{m_-} \frac{1}{\nu_{-0}} . \tag{73}$$

We use, further,

$$T_{d\pm} = \frac{m_\pm v_{d\pm}^2}{2} \quad , \quad \sigma_+ = \frac{\nu_{+-}}{\nu_{+0}} = en\eta\mu_+ \quad , \quad \sigma_- = \frac{\nu_{-+}}{\nu_{-0}} = en\eta\mu_- \quad , \tag{74}$$

and find therewith

$$T_+ = T_{d+}\,\frac{1 + 2\sigma_+\,\frac{v_{d-}}{v_{d+}}}{1 + 2\sigma_+} + T_0\,\frac{1 + 2\sigma_+\,\frac{T_- + T_{d-}}{T_0}}{1 + 2\sigma_+}, \qquad (75)$$

where T_{d-} can be neglected in comparison with T_-.

Before discussing this equation let us derive the corresponding relation for the electrons, using--except for the inelastic collisions, which we do not omit in this case--the simplifications and abbreviations given above. With Eqs. (73) and (74) we arrive at

$$T_- = T_{d-}\,\frac{m_0}{m_-}\left\{1 + \frac{\sigma_-}{1+\sigma_-}\,\frac{v_{d+}}{v_{d-}} + \sum_x \frac{\nu_{0x}/\nu_{-0}}{1+\sigma_-}\left(1 - \frac{eV_x}{2T_{d-}}\right)\right\} +$$

$$+ \frac{T_0}{1+\sigma_-} + \frac{\sigma_-}{1+\sigma_-}\,(T_+ + T_{d+}). \qquad (76)$$

Again this equation can be simplified by making use of

$$\frac{v_{d+}}{v_{d-}} \ll 1; \quad \frac{T_{d-}}{eV_x} \ll 1; \quad \frac{T_{d+}}{T_+} \ll 1. \qquad (76a)$$

Finally, let us study the neutral-particle component. Again the simplifications and abbreviations introduced above may be used except for the omission of the divergence term. For the neutral particles this term is the only source of energy loss within the frame of our discussion (no radiation), and therefore cannot be neglected. Otherwise one would simply calculate the equilibrium temperature of the neutral gas for a given electron and ion temperature. As there are no inelastic collisions we find, using (71a), (73), and (74),

$$T_0 = \frac{T_+ + T_-\,\frac{2m_-\mu_-}{m_+\mu_+}}{1 + \frac{2m_-\mu_-}{m_+\mu_+}} - \frac{\frac{m}{2Rn}\,(n\,\overline{\vec{v}\,v^2})_w}{\frac{\nu_{0+}}{2} + \nu_{0-}}. \qquad (77)$$

The absolute magnitude of the second term, which accounts for the wall losses, is difficult to evaluate. However, it is relatively easy to relate its magnitude to standard discharge conditions without enhanced diffusion. To do so we describe as usual the energy loss at the wall by

$$\frac{m}{R\nu_{0+}} \quad \frac{(n\,\overrightarrow{v}\overline{v^2})_w}{n} = A\,(T_0 - T_w), \tag{78}$$

where T_w is the temperature of the wall. If we let T_∞ and T_{0+} be the standard gas and ion temperatures, respectively, then we find

$$A = \frac{(T_- - T_\infty)\,\frac{2m_-\mu_-}{m_+\mu_+} + (T_{0+} - T_\infty)}{(1 + \frac{2m_-\mu_-}{m_+\mu_+})\,(T_\infty - T_w)} . \tag{79}$$

Introducing Eqs. (78) and (79) into (77) and using the abbreviations

$$a = \frac{m_-\mu_-}{m_+\mu_+} , \qquad \tau = T/T_\infty , \tag{80}$$

we arrive at

$$(1 + 2a)\,\tau_0 = \tau_+ + \tau_-\,2a - \left(\frac{\tau_0 - \tau_w}{1 - \tau_w}\right)\left\{(\tau_{+0} - 1) + 2a(\tau_- - 1)\right\}, \tag{81}$$

which defines τ_0 in terms of τ_+ and τ_-.

Equations (75), (76), and (81) describe the temperature conditions in the discharge.

These equations can be applied in different ways. If one assumes X_z is a given quantity, then (67) allows us to express the drift velocities as functions of X_z, and (75), (76), and (81) may be used to find T_-, T_+, and T_0 as functions of the enhancement parameters σ_-, σ_+.

However, in our present investigation it is more appropriate to consider the electron temperature as a given quantity. Indeed, T_- is prescribed by the requirements of the particle-conservation law and may be evaluated from Eq. (3). With T_- given, the values of T_+ and T_0 as functions of the enhancement parameter σ_+ can be found from (75) and (81).

In application to usual discharge conditions some simplifications of these equations are possible, for instance $\tau_- \gg 1$. Also, as is well known and may be readily verified, the first term in (75) representing the field influence on the ion temperature is negligibly small in comparison with the second term. If we use, further,

$$\sigma_+ = s_+/\sqrt{\tau_+} \quad , \quad a = a \cdot \sqrt{\tau_+} \tag{82a}$$

with

$$a = \frac{m_- \mu_-}{m_+ \mu_+ (T_\infty)} \quad , \quad s_+ = en\eta\mu_+(T_\infty), \tag{82b}$$

we have the following two relations for the ion and gas temperature:

$$\begin{aligned} &\tau_+^{3/2} + \tau_+ \cdot 2 \cdot s_+ - \sqrt{\tau_+}\tau_0 = 2 s_+ \tau_-, \\ &\left(\frac{\tau_0 - \tau_w}{1 - \tau_w}\right) \cdot 2a\tau_- \sqrt{\tau_+} + \tau_0 = \tau_+ + 2a\tau_- \sqrt{\tau_+}. \end{aligned} \tag{83}$$

As T_- is known from Eq. (3) and T_+ and T_0 are known from (83), we may use (76) to find the value of the field X_z. To this end we have to express the drift velocities as functions of the electric field with the help of (67). We multiply Eq. (67) with the unit vector in the z direction. Then, after writing it out for electrons and ions respectively, we can solve for the drift velocities, and find

$$(v_{d\pm})_z = \frac{\mu_\pm}{1 + \sigma_+ + \sigma_-} \quad X_z \, . \tag{84}$$

With the usual assumption that the main drift motion is in the axial direction, we find, by introducing (84) into (76) and making use of (76a), the following relation for the field:

$$X_z^2 = \frac{2 \cdot (1 + \sigma_+ + \sigma_-)^2/\mu_-^2}{m_0 \left\{1 - \sum_x \frac{\nu_{0x}}{\nu_{-0}} \frac{1}{1-\sigma_-} \frac{eV_x}{T_{d-}}\right\}} \cdot \frac{(T_- - T_0) + \sigma_- (T_- - T_+)}{1 + \sigma_-} \, . \tag{85}$$

Equation (85) describes the dependence of X_z on the enhancement parameters.

In this connection it is necessary to make an additional comment on the ratio σ_+/σ_- of these enhancement parameters. From Eq. (74) one should think that the ratio σ_+/σ_- is a constant given by the ratio of the particle mobilities in the neutral gas without ion-electron interaction and without magnetic fields,

$$\frac{\sigma_+}{\sigma_-} = \frac{\nu_{+-}}{\nu_{-+}} = \frac{\mu_+}{\mu_-} \quad . \tag{86}$$

However, this is not correct. As can be seen from the derivations of ν_{+-} and ν_{-+}, the magnitude of this ratio is determined mainly by the persistence of motion in a single electron-ion collision. This persistence factor is very much larger for the ions than for the electrons. However, in the presence of enhanced interaction due to collective phenomena the persistence no longer comes into play. Therefore the ratio σ_+/σ_- may be larger than the value given by Eq. (86) if enhanced interaction is effective.

To demonstrate the effect of enhanced interaction on the temperatures we have calculated τ_+ and τ_0 from (83) for several parameter values,

$$\bar{a} = 2\tau_- a/(1 - \tau_w), \tag{87}$$

and a constant electron temperature $\tau_- = 50$. The result is given in Fig. 6. Clearly, this figure shows that enhanced interaction can cause appreciable increase in the ion temperature and also to some extent in the neutral gas temperature. In particular the ratio T_+/T_- always increases with the enhancement parameter. According to Eq. (26), the parameter $\sigma_- + \sigma_+$ must be larger than unity to cause enhanced diffusion. We do not know what the values of σ_+ and σ_- separately are. However, we would like to stress again that the relation (86) cannot be used. Rather, it is to be expected that with predominant enhancement and therefore decreasing influence of the persistence, the ratio σ_+/σ_- will increase. Under these circumstances an influence on the ion and neutral-gas temperatures can be expected simultaneously with the change in the diffusion rate.

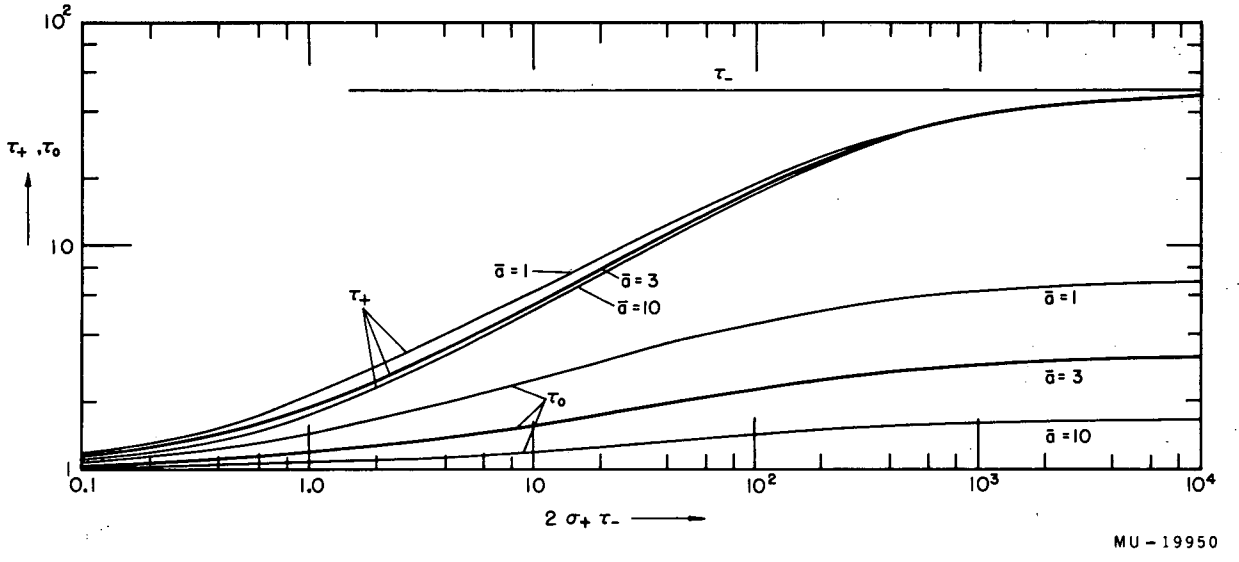

Fig. 6. This figure gives the relative ion (τ_+) and gas (τ_0) temperatures (see eq. 80) as a function of the enhancement parameter $2\sigma_+\tau_-$ for three values of a (see eq. 87) and a constant electron temperature $\tau_- = 50$.

Most interesting is the relation (85) which connects the electric field with the electron temperature $X_z(T_-)$. In general the dependence on the enhancement parameters is rather complicated because of T_+ and T_0. However, under normal conditions ($T_+ \ll T_-$, $T_0 \ll T_-$ and $\sum_x \nu_{0x} eV_x/\nu_{-0} T_{d-} < 1$), X_z is essentially proportional to $(1 + \sigma_+ + \sigma_-)$.

We have stated in Part I that an increase in $D_\perp$ and with that a decrease in the particle loss influences the electron temperature T_- only moderately because of logarithmic dependence and certain numerical factors. This small change in T_- would result in a comparatively small change of X_z, if the classical relation for $X_z(T_-)$, as given by Lehnert[9] were applicable. In this case it would be expected that X_z measurements would not be a sensitive means for detecting enhanced interaction. But using the relation $X_z(T_-)$ as given by (85), one observes that, independent of the particle loss, X_z is strongly affected by the additional energy losses. This makes X_z measurements more promising for the detection of enhanced interaction.

It should be noted, however, that the σ values in this Part III are all average values, and consequently a nonuniform enhancement might still not be detectable from X_z measurements, but could be found from ambipolar potential measurements as described above.

I should like to thank Dr. Thomas K. Allen, Dr. Wulf Kunkel and Dr. Robert V. Pyle for interesting discussions.

This work was done under the auspices of the U. S. Atomic Energy Commission.

Information Division
sa

This report was prepared as an account of Government sponsored work. Neither the United States, nor the Commission, nor any person acting on behalf of the Commission:

A. Makes any warranty or representation, expressed or implied, with respect to the accuracy, completeness, or usefulness of the information contained in this report, or that the use of any information, apparatus, method, or process disclosed in this report may not infringe privately owned rights; or

B. Assumes any liabilities with respect to the use of, or for damages resulting from the use of any information, apparatus, method, or process disclosed in this report.

As used in the above, "person acting on behalf of the Commission" includes any employee or contractor of the Commission, or employee of such contractor, to the extent that such employee or contractor of the Commission, or employee of such contractor prepares, disseminates, or provides access to, any information pursuant to his employment or contract with the Commission, or his employment with such contractor.